

t-SMILES: A Scalable Fragment-based Molecular Representation Framework for De Novo Molecule Generation

Juan-Ni Wu, Tong Wang, Yue Chen, Li-Juan Tang, Hai-Long Wu*, Ru-Qin Yu*

State Key Laboratory of Chemo/Biosensing and Chemometrics, College of Chemistry and Chemical Engineering, Hunan University, Changsha 410082, People's Republic of China

ABSTRACT

Effective representation of molecules is a crucial factor affecting the performance of artificial intelligence models. This study introduces a flexible, fragment-based, multiscale molecular representation framework called t-SMILES (tree-based SMILES) with three code algorithms: TSSA (t-SMILES with Shared Atom), TSDY (t-SMILES with Dummy Atom) and TSID (t-SMILES with ID). It describes molecules using SMILES-type strings obtained by performing a breadth-first search on a full binary tree formed from a fragmented molecular graph. Systematic evaluations using JTVAE, BRICS, MMPA, and Scaffold show the feasibility to construct a multi-code molecular description system, where various descriptions complement each other, enhancing the overall performance. Additionally, it exhibits impressive performance on low-resource datasets, whether the model is original, data augmented, or pre-training fine-tuned. It significantly outperforms classical SMILES, DeepSMILES, SELFIES and baseline models in goal-directed tasks. Furthermore, it surpasses start-of-the-art fragment, graph and SMILES based approaches on ChEMBL, Zinc, and QM9.

¹ State Key Laboratory of Chemo/Biosensing and Chemometrics. College of Chemistry and Chemical Engineering, Hunan University, Changsha 410082, People's Republic of China. Email: rqu@hnu.edu.cn; hlwu@hnu.edu.cn

Introduction

Many molecular descriptors have been used in drug discovery modeling. However, unlike natural language processing (NLP) and image recognition, where deep learning has been shown to excel, one of the domain-specific challenges for artificial intelligence (AI) assisted drug discovery is the lack of a naturally applicable, complete, "raw" molecular representation¹. As molecular representation determines the content, nature and interpretability of the chemical information retained (e.g. pharmacophores, functional groups, physicochemical properties), how the molecule is represented becomes a limiting factor in the performance and explicability of the resulting AI model¹.

In recent years, various deep generative models have been proposed to automatically generate molecules based on different molecular descriptors. Among them, models with sequence representations²⁻⁴, such as Simplified Molecular Input Line Entry System (SMILES)⁵, and 2D representations, such as graphs⁶⁻¹⁰, are the most popular. At the same time, a plethora of models generating molecules in 3D¹¹ also starts to attract attention.

As a relatively more natural representation of molecules, a graph neural network could generate 100% valid molecules as it can easily implement valence bond constraints and other verification rules. However, it has been shown that the expressive power of standard GNNs is bounded by Weisfeiler-Leman (WL) graph isomorphism phenomenon, the lack of ways to model long-range interactions and higher-order structures limited the use of GNNs¹², though some recent studies have proposed new methods such as subgraph isomorphism¹³, message-passing simple networks¹⁴ and many other techniques to improve the expressive power of standard GNNs¹⁵.

SMILES is a linear string obtained by performing a depth-first search (DFS) on a molecular graph. When generating SMILES, parentheses and two numbers must occur in pairs with deep nesting to represent molecular topological structure, such as branches and rings. Models trained on SMILES generate some chemically invalid strings, especially when trained on small datasets. Although it is a straightforward task to select valid strings for output, the critical concern is that these invalid strings indicate that even state-of-the-art (SOTA) deep learning models struggle with accurately comprehending SMILES syntax and semantics, which is mainly caused by unbalanced parentheses and ring identifier. Furthermore, it is uncertain what kind of chemical information could be learned from such models. This is considered as a limitation that needs to be addressed¹⁶.

Two alternative solutions to the classical SMILES have been proposed later. DeepSMILES(DSMILES)¹⁷ resolves most cases of syntactical mistakes caused by long-term dependencies. However, it still allows for semantically incorrect strings, such as 'CO=CC' (the oxygen atom that has three bonds - a violation of the maximum number of bonds that neutral oxygen can form), and some studies indicate that the advanced grammar has a detrimental effect on the learning capability in some specific tasks^{18,19}. Self-referencing embedded strings (SELFIES)²⁰ is an entirely different molecular representation, in which every SELFIES string specifies a valid chemical graph. However, the approach's focus on robustness can make certain SELFIES more challenging to read¹⁹.

SMILES, DSMILES and SELFIES are all atom-based linear representations. Compared with atom-based techniques, the search space is significantly reduced by using the fragment strategy. In addition, fragments could provide fundamental insights into molecular recognition, for example, between proteins and ligands. Consequently, there is a higher probability of finding molecules that match the known targets. Currently, almost all fragment (motif or substructure) based deep learning²¹ methods published rely on a specific substructure dictionary of candidate fragments^{9,22-28}. It is obvious that dictionary-ID-based models suffer from some fundamental problems such as in-vocabulary (IV), out-of-vocabulary (OOV), and high-dimensional sparse representation (curse of dimensionality). Although deep learning has been widely used in molecular generation tasks^{29,30} with the fragment-based method, the approach of fragmenting molecules and encoding molecular substructures as a string-type sequence to finally generate new molecules has not yet been thoroughly explored.

Jean-Marie Lehn's famous quotation "Atoms are letters, molecules are the words, supramolecular entities are the sentences and the chapters"^{31,32} was cited by the researchers³³ studying the rank distribution of fragments in organic molecules being similar to that of words in the English language. This idea inspired us to select the classical SMILES as the starting choice for fragment description and adopt advanced NLP methodologies to handle fragment-based molecular modeling tasks, which could hybridize the advantages of graph model paying more attention to molecular topology structure and language model (LM) having powerful learning ability.

Therefore, we propose a new molecule description framework called t-SMILES based on the fragmented molecule, which describes a molecule with a classical SMILES-type string and can take the sequence-based models as the primary generation model. This study introduces three t-SMILES code algorithms: TSSA, TSDY and TSID, *vide infra*.

The newly proposed t-SMILES framework first generates an acyclic molecular tree (AMT) whose role is to represent fragmented molecules. The AMT is transformed into a full binary tree (FBT) in the second stage. Finally, the breadth-first traversal of the FBT yields a t-SMILES string.

Compared to SMILES, t-SMILES introduces only two new symbols, "&" and "^", to encode multi-scale and hierarchical molecular topologies. So, the t-SMILES algorithm provides a scalable and adaptable framework that is theoretically capable of supporting a broad range of substructure schemes, as long as they generate chemically valid fragments and produce valid AMT. Moreover, owing to its multiscale and hierarchical representation, the model based on t-SMILES is capable of learning high-level topology structural information while processing detailed substructure information. Notably, the t-SMILES algorithm can construct a multi-code system for molecule description. In this system, classical SMILES can be integrated as a special case termed TS_Vanilla, and multiple descriptions can collaborate to improve comprehensive performance.

Well-trained string-based language models have proven effective in various studies. The performance discrepancies between various codes heavily depend on their underlying disparities. Consequently, we methodically assess t-SMILES by initially delving into its distinctive features. Subsequently, we conduct experiments on two labeled low-resource datasets, JNK3³⁴ and AID1706³⁵. Our investigation focuses on t-SMILES and its substitutes' limitations, achieved via utilization of standard, data augmentation, and pre-training fine-tuning models. In line with our goal, we evaluate twenty goal-directed tasks on ChEMBL in parallel. We also thoroughly experiment on ChEMBL, Zinc, and QM9, via comparison between t-SMILES models and their alternatives using similar settings. Additionally, we compare various baseline models and the most prevalent graph neural network models. Lastly, an ablation study is carried out to confirm the efficacy of the generative model based on SMILES with reconstruction. In order to evaluate the adaptability and flexibility of t-SMILES algorithm, four previously published fragmentation algorithms were utilized to break down molecules, including JTVAE⁸, BRICS³⁶, MMPA³⁷ and Scaffold³⁸. Distribution-learning benchmarks, goal-directed benchmarks, and Wasserstein distance metrics for physicochemical properties are used in different experiments.

Detailed comparative experiments demonstrate the potential of t-SMILES models to achieve 100% theoretical validity and generate highly novel molecules, outperforming start-of-the-art (SOTA) SMILES-based models. Compared to SMILES, DSMILES, and SELFIES, the overall solution of t-SMILES can outmaneuver overfitting problem and significantly

enhances balanced performance on low-resource datasets, regardless of whether data augmentation or pretrain fine-tuning models are used. In addition, t-SMILES models are proficient in capturing the physicochemical properties of molecules, ensuring that the generated molecules maintain similarity to the training molecule distribution. This results in significantly improved performance compared to fragment-based and graph-based baseline models. In particular, t-SMILES models with goal-directed reconstruction algorithm show considerable benefits over SMILES, DSMILES, SELFIES and SOTA CReM³⁹ in goal-oriented tasks.

Recently, pre-trained Transformers⁴⁰ based LMs have demonstrated their ability to generate text that closely resembles human writing. Furthermore, as interest grows in treating larger and more complex molecules, language models may outperform most graph generation models in learning these complex molecules⁴¹. Although current de novo molecular generation models have made significant progress, we hope that scalable t-SMILES could introduce exciting opportunities for AI-assisted molecular modeling.

Methods

To support the t-SMILES algorithm, we introduce a new character, '&', to act as a tree node when the node is not a real fragment in FBT. Additionally, we introduce another new character, '^', to separate two adjacent substructure segments in t-SMILES string, similar to the blank character in English sentences that separates two words.

In this section, we begin by outlining the fundamental concept of t-SMILES. Subsequently, we highlight FBT and AMT, which constitute the key components of the t-SMILES algorithm. Next, we briefly introduce molecular fragmentation algorithms and molecular reconstruction strategy.

t-SMILES Algorithm Overview

In the t-SMILES algorithm, a molecular graph is firstly divided into valid chemical fragments (or substructures, clusters, subgroups, subgraphs) using one specified disconnection method or some hybrid disconnection methods to obtain its AMT shown in the middle of Fig.1. Following with the AMT being transformed into a FBT, and finally the FBT is traversed in breadth-first search (BFS) to obtain the t-SMILES string. During the reconstruction, the reverse process is used, and finally the molecular fragments are assembled into the chemical correct molecular graph.

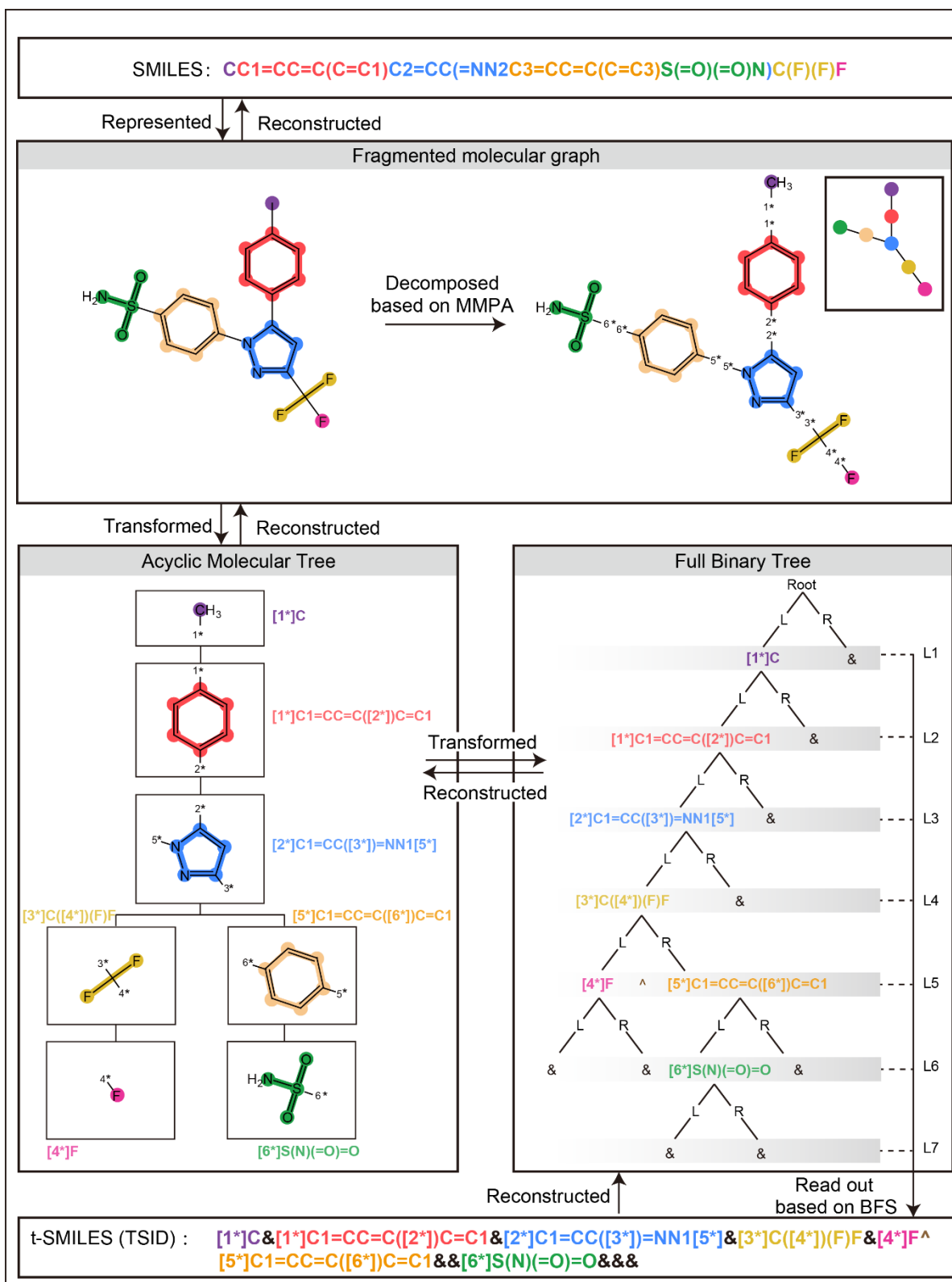


Fig.1 Overview of the t-SMILES algorithm: The molecular graph is first decomposed using selected molecular fragmentation algorithm to build an AMT, which is then transformed into an FBT. Finally, the BFS algorithm is used to traverse the FBT and obtain its t-SMILES string. To reconstruct the molecule, rebuilding the FBT from the t-SMILES string, transforming it to an AMT, and finally assembling the AMT back into the original molecule. In TSID, the dummy atom and its id [n*] are used to indicate joint point. When the IDs are removed from the TSID code, the TSDY code is created. New symbol '&' is used to mark empty tree nodes. In L5, new symbol '^' is used to separate two SMILES pieces in t-SMILES string. TSSA uses a different way to get pieces, please see SI.A.1 for the entire process and more examples. MMPA is used as an example in both figures to cut molecules.

Algorithm steps to construct t-SMILES from a molecule

Step 1: Break down a molecule according to the selected molecular fragmentation algorithm to build AMT;

Step 2: Convert the AMT to a FBT;

Step 3: Traverse the FBT with BFS algorithm to get t-SMILES.

The BFS algorithm for the tree is a level-order traversal of tree. For any node *w* in the BFS tree rooted at *v*, the tree path from *v* to *w* in the tree corresponds to a shortest path from *v* to *w* in the corresponding graph. Please refer to SI.A.2 for a demonstration of the BFS algorithm.

Three coding algorithms are presented in this study:

- 1) TSSA: t-SMILES with shared atom.
- 2) TSDY: t-SMILES with dummy atom but without ID.
- 3) TSID: t-SMILES with ID and dummy atom.

The distinction between TSSA and TSDY/TSID is that in TSSA, two fragments share a real atom as a connecting point, whereas TSDY and TSID use a dummy atom (indicated by character '*' with or without ID) to illustrate how the group bonds. TSDY and TSID have a simpler fragmentation and assembling logic compared to TSSA, as can be seen in Fig.1 and Supporting Information (SI) SI.A.1. For additional examples and more detailed information on the various code algorithms, please refer to SI.A.1.

For example, in Fig 1 and SI.Fig.A.1.1, the three t-SMILES codes of Celecoxib are:

- 1) TSID_M (Fig.1):

```
[1*]C&[1*]C1=CC=C([2*])C=C1&[2*]C1=CC([3*])=NN1[5*]&[3*]C([4*])(F)F&[4*]F^[5*]C1=CC=C([6*])C=C1&&[6*]S(N)(=O)=O&&&
```

- 2) TSDY_M (Fig.1, replace [n*] with *):

```
*C&*C1=CC=C(*)C=C1*C1=CC(*)=NN1*&*C*(F)F*F^*C1=CC=C(*)C=C1&&*S(N)(=O)=O&&&
```

- 3) TSSA_M(SI.Fig.A.1.1):

```
CC&C1=CC=CC=C1&CC&C1=C[NH]N=C1&CN&C1=CC=CC=C1^CC^CS&C&N[SH](=O)=O&CF&&&&FCF&&
```

Full Binary Tree

Tree is the core concept in proposed t-SMILES algorithm. A tree is a special type of graph in which there is just a single path connecting each pair of vertices, that is, there are no cycles or rings within the graph. The root node of a tree is the starting point while the other vertices are either branch nodes or leaf nodes.

A FBT is a special type of binary tree in which every parent node/internal node has either two or no children. As the most trivial tree, FBT's structure is regular and easy to calculate. The reason for using FBT with some redundant nodes instead of complete binary tree or other

trees is that its algorithm and structure being easy to learn by deep learning models, and the redundant nodes could be used as global marker nodes. In this work, the character '&' (tree node marked as '&') marks the end of the tree branch in the FBT, capable of providing the global structural information describing the molecular topology in the t-SMILES string.

With chemically meaningful molecular fragmentation representation using FBT, t-SMILES effectively reduces the nesting depth of brackets in SMILES codes, weakens the long-term dependencies in grammar, and fundamentally reduces the difficulty of learning molecular information using sequence-based deep learning models. In t-SMILES algorithm, except for the extra two characters '&' and '^', no more symbols are introduced, nor are recursion and other sophisticated calculations with high computational complexity introduced.

Molecule Decomposition

According to Lounkine *et al.*⁴², there exist four major strategies to fragment designing: knowledge-based, synthetically oriented, random, and systematic or hierarchical. The open-source molecular toolkit RDKit⁴³ has implemented some molecular fragmentation methods, such as BRICS³⁶, MMPA(Matched Molecular Pair Analysis)³⁷, and Scaffold³⁸, etc. Another type of molecular decomposition algorithm in our study could find its root in feature tree⁴⁴ published for molecular similarity algorithm by Rarey *et al.* in 1998 and JTVAE⁸ proposed later by Jin *et al.*

The first step in the t-SMILES algorithm involves decomposing molecules into valid chemical fragments, utilizing a specified disconnection algorithm. And then generating a reduced graph^{45,46} according to the cutting-off logic of fragmentation algorithms and then calculate its spanning tree as AMT.

Acyclic Molecular Tree

The idea of using tree as the base data structure of algorithms to address molecular related tasks has been long established in cheminformatics. In early study of molecular descriptor and similarity analysis, algorithms such as reduced graph^{45,46}, feature tree^{44,47} not only had shown potential power to improve the similarity search but also being capable of retrieving more diverse active compounds than using Daylight fingerprints⁴⁸. Some recent works⁴⁹⁻⁵⁰ proposed to incorporate tree-based deep learning models into molecular generation and synthesis tasks as well.

AMT being capable to describe the molecule at various levels of resolution, reduced graph⁴⁵ provides summary representations of chemical structures by collapsing groups of

connected atoms into single nodes while preserving the topology of the original structures. In reduced graph, the nodes represent groups of atoms and the edges represent the physical bonds between the groups. Constructing reduced graph in this way forms a hierarchical graph, whose top layer being the molecular topology representing global information, and the bottom layer representing molecular fragments of detailed information. Groups of atoms are clustered into a node in the reduced graph approach, which could be done based on fragmentation algorithms. The feature tree⁴⁴ is a representation of a molecule similar to a reduced graph. The vertices of the feature tree are molecular fragments and edges connect vertices that represent fragments connected in the simple molecular graph. In t-SMILES algorithm, the minimum spanning tree of the reduced graph and the concept of feature tree could be regarded as an AMT in the intermediate step, and then the next encoding algorithm is done based on this AMT.

Specific to our experiments, one part of the approach is to generate AMT based on the tree logic fragmented by the BRICS, MMPA, and Scaffold. Another method uses a junction tree introduced by Jin *et al.* in JTVAE⁸ as the AMT.

Molecular Reconstruction

We follow the following steps to reconstruct molecules from t-SMILES strings.

Step 1: Decompose t-SMILES string to reconstruct the FBT;

Step 2: Convert the FBT to the AMT;

Step 3: Assemble molecular fragments according to the selected algorithm to generate the correct molecular graph and then optimize it.

During reconstruction, one key problem is how to assemble the molecular fragments together to get a ‘chemically correct’ molecule. In this study, for efficiency reasons, we assemble molecular graph one neighborhood at a time, following the order in which the tree itself was generated. In other words, we start from the root node of AMT and its neighbors, then we proceed to assemble the neighbors and their associated clusters, and so on. If there is more than one candidate when assembling two pieces, we select one molecule based on some specific rules, such as randomly or using a goal-directed function defined in GuacaMol⁵¹.

Assembling fragments to create a chemically valid molecule is a challenging task with a significant impact on the quality of molecules. Some algorithms such as Monte Carlo tree search (MCTS), CReM³⁹ can serve as a starting points for future research in this field.

Results

First, we investigate the distinctive features of t-SMILES from different research perspectives. Then, we conduct rigorous and systematic experiments. For the t-SMILES family,

various singleton and hybrid strategies can be used to accomplish distinct goals in a range of ways. Due to limited computational resources, we evaluate TSSA and TSDY individually in two goal-oriented tasks. TSSA codes undergo evaluation in labeled datasets JNK3 and AID1706 as part of a goal-oriented task with limited resources. TSDY codes are evaluated in twenty goal-directed benchmarks according to the specifications described in GuacaMol⁵¹. Furthermore, we carry out systematic experiments to evaluate singleton and hybrid TSSA, TSDY, and TSID models on ChEMBL, ZINC, and QM9. In addition, baseline models based on SMILES, DSMILES, SELFIES, SMILES-augmentation, and transfer learning are presented and compared.

SI.Table.B.1 presents a preliminary summary of t-SMILES coding algorithms and experiments. In SI.E.8, we report a brief study on ring-opening problem using TSID. SI.D.8 outlines the results of an ablation study. For more detailed information on experimental configurations and evaluation metrics, please refer to section SI.B.

Distinguished properties of t-SMILES

The training data includes essential information for appropriate deep learning algorithms. This section presents a concise summary of the token distribution and nesting depth for SMILES, DSMILES, SELFIES and t-SMILES, serving as a useful reference for future research.

Token Distribution LM uses probability and statistical techniques to calculate the possibility of word sequences in sentences and then do estimation⁵². Although t-SMILES introduces just two extra characters, "&" and "^," its token distribution differs entirely from SMILES. The distribution of tokens on Zinc is shown in Fig.2, more detailed information in the SI.C.1.

Fig.2 shows that the proportions of the characters '(' and ')' in t-SMILES codes are all less than 5%(TSSA_J:0.008%, TSSA_B:4.3%, TSSA_M:0.8%, TSSA_S: 4.2%). In comparison, the proportions of characters '(' and ')' are more than 10% in SMILES-based code. On the other hand, the distribution shows that the symbols '&^', which are used to indicate the molecular topology structure in t-SMILES but do not have to be in pairs, have the second highest frequency in the TSSA codes, just below the frequency of 'C'. The similarities and differences between t-SMILES and SMILES indicate that, a crucial task of the SMILES model is to learn and predict PAIRED '(' and ')' symbols. Conversely, the t-SMILES model must learn how to reason NON-PAIRED symbols '&' and '^'.

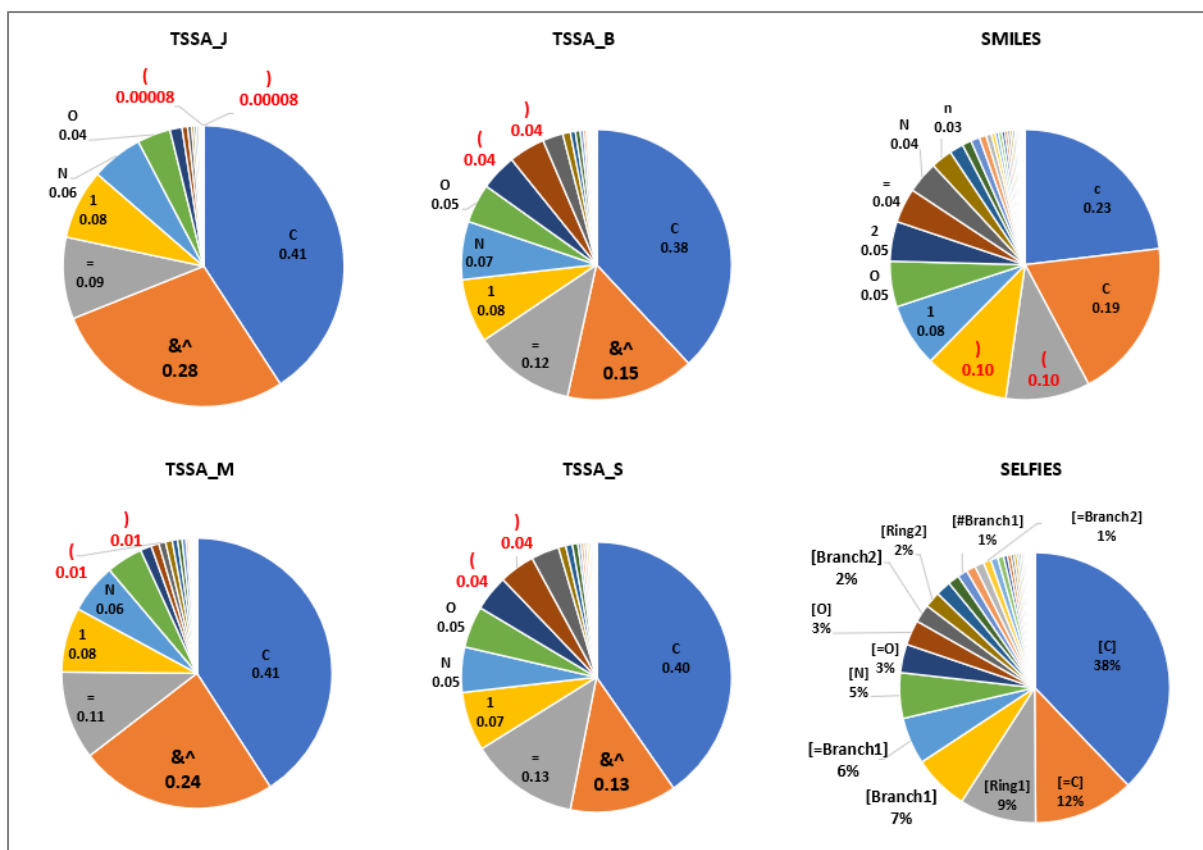


Fig.2 Distributions of tokens for TSSA codes, SMILES and SELFIES

Nesting Depth How deep learning models such as LSTM⁵³ or Transformer⁴⁰ learn long-term dependencies is one of the driving forces behind the development of NLP. In classical SMILES, deeply nested pairs of characters, such as '(' and ')', are the key tokens to mark the rings and branches of molecules, which are also one of the main reasons why the generated string could not be decoded into a chemically valid molecule. Although SMILES is still used to represent molecular substructure, t-SMILES abandons the algorithm of depth-first traversal of molecular trees, which fundamentally reduces the depth of nesting and the proportion of characters that must appear in pairs. For example, the TSDY_M code on ChEMBL increases the proportion of the 0-1-2 nesting depth from 68.006% to 99.270%, while decreasing the 3-4-5 nesting depth from 31.886% to 0.730%, and the 6-11 nesting depth from 0.108% to 0.00019%. The detailed statistical data on the nesting depth of ChEMBL and Zinc are listed in SI.C.2.1 to SI.C.2.3, respectively.

Reconstruction and Generative model without training

MOG⁵⁴ argued that the common "pitfall" of existing molecular generative models based on distributional learning is that exploration is limited to the training distribution, and the

generated molecules exhibit "striking similarity" to molecules in the training set. The author notes that: models that do not require training molecules are free from this problem, but they introduce other problems such as long training time, sensitivity to the balance between exploration and exploitation, large variance, and most importantly, lack of information about the known distribution. From this point of view, t-SMILES provides a comprehensive solution by integrating distributional and non-distributional learning into a single system, thereby circumventing the aforementioned "pitfall".

The overall performance of t-SMILES model is determined by two primary factors: 1) the model's ability to efficiently learn and generate t-SMILES strings, and 2) the effectiveness of the reconstruction and molecular optimization algorithm. In t-SMILES, novel molecules can be generated by direct reconstruction of FBT without training. If we output all possible assembly results, we could generate a group of molecules from a set consisting of several molecular fragments with different structures. From this point of view, generating new molecules with the desired structure (desired properties) rather than duplicating the training set is the potential goal of the molecule generation task and not a negative aspect. The results of the random reconstruction on ChEMBL, Zinc and QM9 are shown in Table 1 and S.I.E.1-3.

Tables and figures show that the direct reconstruction algorithm effectively preserves the physiochemical properties of the original dataset, as demonstrated by significantly high KLD and FCD values across all three datasets. In addition, the uniqueness and novelty scores for TSSA on ChEMBL and Zinc exceed 0.5 for all four decomposition algorithms, suggesting that the reconstruction algorithm can serve as an efficient generation model without training.

Although novelty scores for TSDY have intentionally been reduced, it is still possible for TSDY to function as a generation model without training in certain conditions. However, in order to build a deep neural network based generative model, it is needed for TSID to undergo training. Despite the theoretical TSID reconstruction novelty score being zero, our attempts to represent molecules in the Kekulize style resulted in scores of 0.004 and 0.010 on ChEMBL and Zinc. It is challenging to convert particular fragments and molecules into Kekule style using RDKit. This issue does not pose a problem for generative models, but we are actively working to enhance it for retrosynthesis and reaction prediction.

Table 1. Results by directly reconstructing molecules using random reconstruction algorithm.

Code Algorithm	Dataset	Model	Valid	Unique	Novelty	KLD	FCD	FBTs
TSSA	ChEMBL	TSSA_J	1.000	0.786	0.677	0.969	0.694	5029
		TSSA_B	1.000	0.782	0.538	0.974	0.715	610633
		TSSA_M	1.000	0.783	0.681	0.980	0.815	88938
		TSSA_S	1.000	0.785	0.700	0.963	0.802	515329
	Zinc	TSSA_J	1.000	0.770	0.662	0.982	0.811	61786
		TSSA_B	1.000	0.776	0.603	0.970	0.735	1197
		TSSA_M	1.000	0.778	0.679	0.984	0.843	18989
		TSSA_S	1.000	0.783	0.709	0.960	0.835	485
	QM9	TSSA_J	1.000	0.741	0.245	0.976	0.968	279
		TSSA_B	1.000	0.750	0.044	0.997	0.981	32
		TSSA_M	1.000	0.727	0.108	0.997	0.976	238
		TSSA_S	1.000	0.717	0.119	0.996	0.972	69
TSDY	ChEMBL	TSDY_B	1.000	0.996	0.210	0.997	0.915	4267
		TSDY_M	1.000	0.996	0.711	0.987	0.897	85409
		TSDY_S	1.000	0.996	0.459	0.995	0.913	39
	Zinc	TSDY_B	1.000	0.978	0.365	0.995	0.909	190
		TSDY_M	1.000	0.978	0.688	0.996	0.916	5681
		TSDY_S	1.000	0.978	0.393	0.997	0.939	18
TSID	ChEMBL	TSID_B	1.000	0.996	0.004	0.998	0.925	4267
	Zinc	TSID_B	1.000	0.978	0.010	0.999	0.945	190

Chemical space exploration and Data augmentation for t-SMILES

One of the fundamental motivation for using fragments is their ability to sample the chemical space efficiently⁵⁵. In t-SMILES system, training data can be augmented from four levels: 1) decomposition algorithm, 2) reconstruction, 3) enumeration of fragment strings and 4) enumeration of FBTs.

Different molecular segmentation algorithms divide a molecule in various ways, resulting in distinct segment groups. Subsequently, these segment groups cover different chemical spaces when producing new molecules. Refer to S.I.C.3 and S.I.G for information on physicochemical properties and atom environment substructure. The chemical space for t-SMILES is illustrated through the reconstruction of FBTs using TSSA code algorithms for a single molecule, as demonstrated in S.I.C.4.

In terms of data augmentation, forming new and different samples from the training dataset can improve the performance and results of a machine learning model. Recent evidence suggests that SMILES enumeration may be a valid way to augment the data in a "small" dataset in order to improve the quality of generative models¹⁸. However, Skinnider *et al.*¹⁶ argue that 'over-enumeration' in large datasets of structurally complex molecules, where even small amounts of data augmentation can have a negative impact on performance.

Due to the fact that the enumerated strings represent the same molecules, the data augmentation method implemented by enumerating SMILES cannot access a larger chemical space in the real chemical sense, but it is possible to provide more strings for the deep learning model to learn the SMILES syntax. Of course, the skills used to augment SMILES string can also be used to augment t-SMILES string at the fragment level, since SMILES is used to describe the fragments in t-SMILES. In addition, similar to the enumeration of SMILES, t-SMILES can be enumerated using different fragments as the root when generating FBT. Compared to SMILES, if we use reconstruction as a data augmentation method for t-SMILES, the later would generate different molecules from the same set of fragments. As a result, a broader space could be easily accessed in the chemical sense.

Experiments on Low-Resource Datasets

The scarcity of labeled data presents a challenge for implementing deep learning in target-oriented drug discovery. Additionally, generative models that rely on distributional learning tend to learn the distribution of the training data. Furthermore, when limited training data is used, deep learning models are prone to overfitting, resulting in reduced generalization performance of the model. For these reasons, we only use active molecules as training data in this section to investigate the overfitting problem and explore the active chemical space.

A discrimination model based on AttentiveFP⁵⁶ is trained to predict whether the newly generated molecules are active. For JNK3, the ROC_AUC values of this AttentiveFP discrimination model are as follows: training: 0.995, validation: 0.980, and testing: 0.989.

We evaluate two low-resource datasets: JNK3 with 923 active molecules and AID1706 with only 329 active molecules. Please reference SI.D.1 and SI.D.11 for a comparison of active and inactive molecules. The figures indicate that AID1706 presents more challenges than JNK3. Nonetheless, TSSA_S models exhibit significantly higher novelty scores than SMILES. Please see SI.D.9-11 for the experimental results of AID1706.

Overfitting problem on JNK3 To investigate the overfitting problem against different algorithms on JNK3, we first train generative models with different training epochs for SMILES, DSMILES, SELFIES, and t-SMILES. In addition, data augmentation and pre-train fine-tune based models are also trained on SMILES and t-SMILES. See Table 2, Fig.3 SI.Fig.D.5, Fig.4.J1-2 and SI.D for detailed experiment results.

Table 2. Results on JNK3 active molecules using MolGPT with different training epochs.

Model3	Valid	Novelty	FCD	Active Novel	FBT Novel	Frag Novel
SMILES[R200]	0.795	0.120	0.584	0.072	N/A	N/A
SMILES[R2000]	1.000	0.001	0.765	0.004	N/A	N/A
DSMILES[R200]	0.677	0.076	0.510	0.043	N/A	N/A
DSMILES[R2000]	0.999	0.001	0.778	0.001	N/A	N/A
SELFIES[R200]	1.000	0.238	0.544	0.148	N/A	N/A
SELFIES[R2000]	1.000	0.008	0.767	0.050	N/A	N/A
TSSA_S[R300]	1.000	0.833	0.564	0.582	2.655	0.962
TSSA_S[R5000]	1.000	0.817	0.608	0.564	2.534	0.049
TSSA_S[R50000]	1.000	0.824	0.572	0.571	2.379	0.023
TSSA_HSV[R200]	1.000	0.827	0.483	0.961	0.680	0.350
TSSA_HSV[R2000]	1.000	0.447	0.716	0.319	1.810	0.365
TSSA_H6[R200]	1.000	0.896	0.683	0.947	0.622	0.374
TSSA_H6[R2000]	1.000	0.657	0.619	0.437	2.672	23.745
TF_SMILES[R5]	0.887	0.707	0.523	0.526	N/A	N/A
TF_SMILES[R100]	0.999	0.033	0.764	0.023	N/A	N/A
TF_TSSA_S[R5]	1.000	0.932	0.483	0.710	2.897	9.105
TF_TSSA_S[R100]	1.000	0.849	0.570	0.569	2.431	0.208
SMILES_Aug50[R10]	0.807	0.570	0.566	0.483	N/A	N/A
SMILES_Aug50[R100]	0.995	0.049	0.750	0.047	N/A	N/A
TSSA_S_Rec50[R10]	1.000	0.962	0.389	0.829	2.414	1.757
TSSA_S_Rec50[R100]	1.000	0.960	0.411	0.809	2.448	0.655

*‘Active Novel’ means the newly generated novelty molecules predicted by the AttentiveFP model as active. ‘FBT’ means different FBTs compared with the training dataset. ‘R’ means training epochs. ‘Aug’ means augmenting training dataset by enumerating SMILES. ‘Rec’ means reconstructing directly from active molecules to generate new active molecules. ‘TF’ means transfer learning. See SI.D.3 and SI.D.4 for more detailed results.

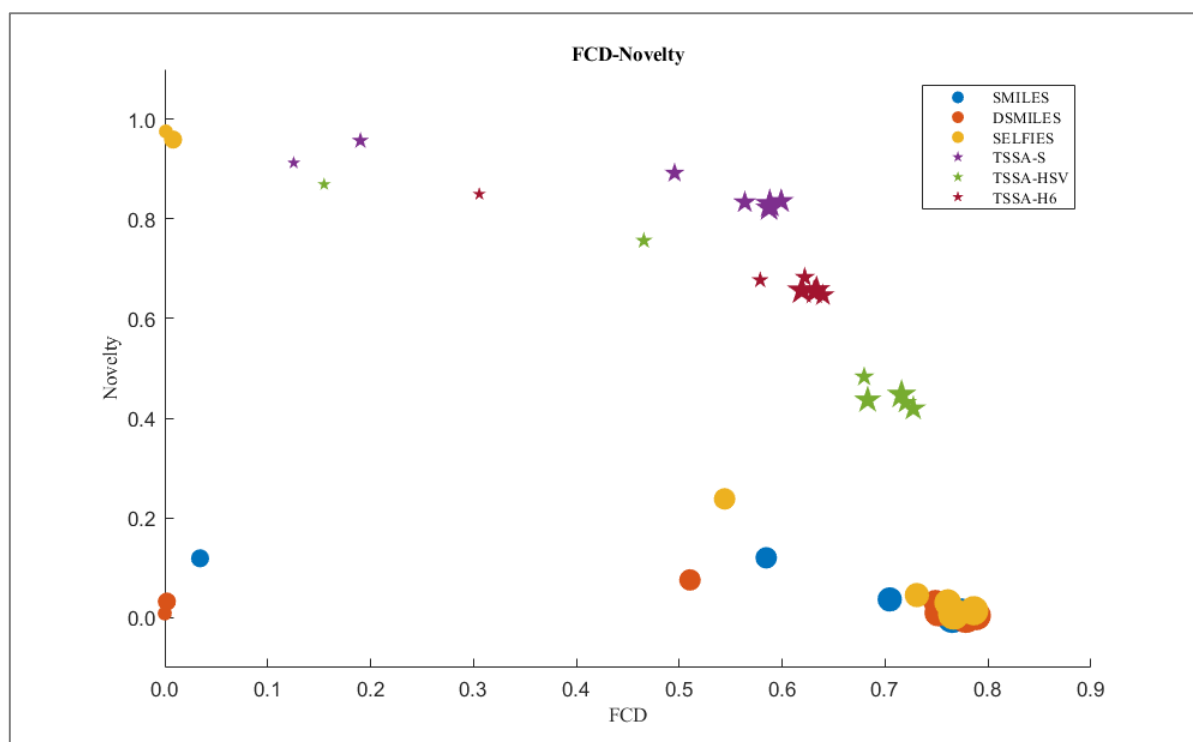


Fig.3 Novelty and FCD scores against SMILES, DSMILES, SELFIES, TSSA, TSSA_HSV(Hybrid model on TS_Vanilla and TSSA_S) and TSSA_H6(Hybrid all TSSA codes)on different training epochs. Seven data points from small to large for each code indicate the number of training epochs:50, 100, 200, 300, 500, 1,000, and 2,000 respectively.

Overall, the models based on SMILES, DSMILES, SELFIES, and t-SMILES show a consistent increase in FCD scores with the increasing number of training iterations. Notably, after the 200th training epoch, the FCD curves of SMILES, DSMILES, and SELFIES surpass that of t-SMILES in SI.Fig.D.5 and subsequently stabilize independently. Additionally, the data presents a significant negative correlation between novelty and FCD scores.

In detail, the novelty scores of SMILES and DSMILES initially increase, but then sharply decline after 200 training epochs and eventually almost reach zero. SELFIES model experiences an abrupt drop in novelty score at the 200 epochs, also falling to almost zero. In contrast, t-SMILES's novelty score initially fluctuates slightly, but then stabilizes at a value of approximately 0.8. The hybrid t-SMILES models surpass all t-SMILES models in FCD scores. Additionally, they attain notably higher novelty scores and marginally lower FCD scores than the SMILES, DSMILES, and SELFIES models.

Regarding the notably high novelty scores during the 50th and 100th training epochs of SELFIES, this is because the SELFIES algorithm always transforms the generated strings into valid molecules. However, at these points, the FCD scores nearly approach zero, indicating that the newly produced molecules are vastly different from the training dataset. Refer to SI.D.7 for the variously produced molecules during differing training epochs.

Systematic experiments indicate that the special multiscale coding algorithm and reconstruction philosophy employed by t-SMILES effectively circumvent the overfitting problem on datasets with limited resources. To achieve a desired distribution of molecules in real-world experiments, selecting an appropriate training epoch to balance both FCD and novelty scores is essential. See SI.D.5 for more comments.

Besides that, in transfer learning scenario, when the number of training epochs is increased from 5 to 100, the active novelty score of the t-SMILES-based model decreases from 0.710 to 0.569. However, the SMILES-based model experiences a drastic drop from 0.526 to 0.023

When analyzing the models based on data augmentation, an increase in the number of training epochs from 10 to 100 leads to a striking decrease in active novelty score for the SMILES-based model - from 0.483 to 0.047. Nevertheless, the t-SMILES based models preserve their high levels of active novelty scores, reaching 0.829 and 0.809 respectively, with only slight decreases.

The statistical data suggests that utilizing data augmentation or pre-trained models could be more beneficial for SMILES model with limited resources. However, a conventional TSSA_S model may achieve better results compared to models using SMILES-based data

augmentation and transfer learning techniques. t-SMILES-based transfer learning models achieved the highest scores among all models.

This experiment also indicates that the t-SMILES algorithm can build a multi-code system for molecular description, in which each decomposition algorithm acts as a kind of chemical word segmentation algorithm splitting a molecule as different strings. All of these codes complement each other and contribute to a mixed chemical space. If one code is insufficient for inference, another code can provide complementary information. In this framework, classical SMILES can be unified as a special case of t-SMILES to achieve better-balanced performance using hybrid decomposition algorithms.

Distribution Learning on JNK3 For detailed results on distribution learning, including TSSA_J, TSSA_B, and TSSA_M, please refer to S.I.D.3 and S.I.D.4.

Compared to classical SMILES and DSMILES, t-SMILES and SELFIES based models generate actually 100% valid molecules. On the other hand, the t-SMILES model achieved higher uniqueness and novelty scores with almost similar KLD scores compared to SMILES, DSMILES and SELFIES. For data augmentation and transfer learning, t-SMILES based models also achieve higher uniqueness and novelty scores. Among the statistical data, the highest novelty score of 0.962 comes from mode TSSA_S_Rec50[R10].

Physicochemical Properties on JNK3 Detailed distributions of physicochemical properties on S.I.D.6 and Fig.4.J1-2 indicate that the SELFIES model requires further optimization to match the performance of SMILES. Although the t-SMILES family outperforms SMILES in producing more active molecules, we recommend using a hybrid model to produce high-quality molecules. Furthermore, it is worth noting that TSDY and TSID can provide a more accurate representation of physicochemical properties compared to TSSA. Therefore, these alternatives could be considered for future research.

Experiments on ChEMBL

Distribution Learning on ChEMBL As shown in Table 3, t-SMILES based models outperform Graph MCTS, hgraph2graph(hG2G), and SOTA graph mode MGM. It seems difficult for Graph MCTS to capture the properties of the dataset distributions as shown by its almost-zero FCD score.

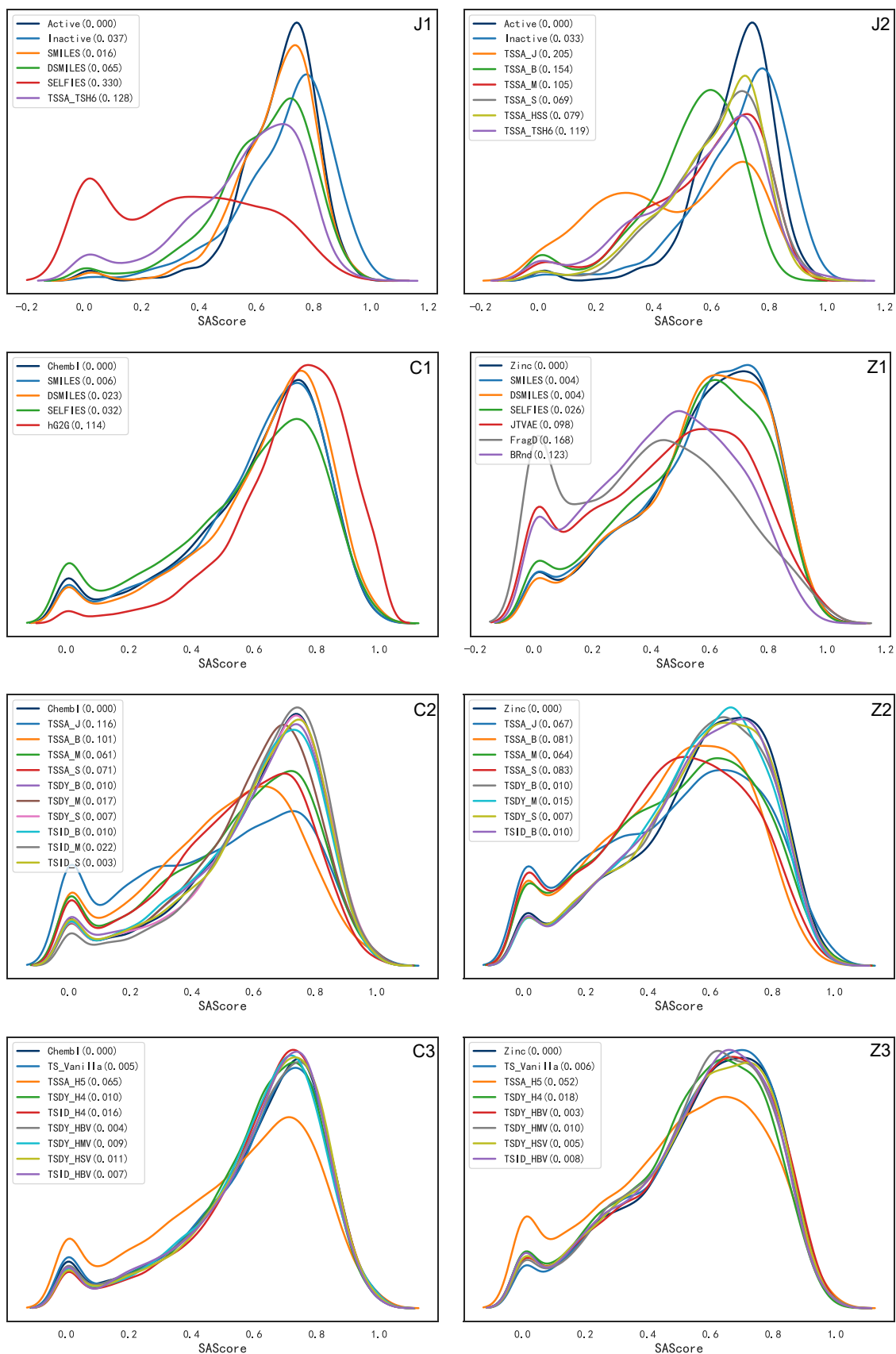


Fig.4 SAScore of JNK3, ChEMBL and Zinc. For more detailed pictures, please refer SI.D and SI.E.

J1 and J2: Baseline and t-SMILES models on JNK3.

C0, C1 and C2: Baseline, Singleton t-SMILES and Hybrid t-SMILES models on ChEMBL.

Z0, Z1 and Z2: Baseline, Singleton t-SMILES and Hybrid t-SMILES models on Zinc.

Table 3. Results for the Distribution-Learning Benchmarks on ChEMBL using GPT.

	Model	Valid	Unique	Novelty	KLD	FCD	Nov./Uni.
Baseline Graph	Graph MCTS ^{10,51}	1.000	1.000	0.994	0.522	0.015	N/A
	hG2G ⁹	1.000	0.994	0.940	0.870	0.485	N/A
	MGM ⁷	0.849	1.000	0.722	0.987	0.845	N/A
Baseline SMILES	LSTM ^{53,51}	0.959	1.000	0.912	0.991	0.913	N/A
	CharacterVAE ^{2,51}	0.870	0.999	0.974	0.982	0.863	N/A
	AAE ^{57,51}	0.822	1.000	0.998	0.886	0.529	N/A
	ORGAN ^{3,51}	0.379	0.841	0.687	0.267	0.000	N/A
	Transformer Reg ^{40,7}	0.961	1.000	0.846	0.977	0.883	N/A
	MolGPT ⁴	0.981	0.998	1.000	0.992	0.907	N/A
String	SMILES_[R10]	0.977	0.767	0.709	0.990	0.890	0.924
	DSMILES_[R10]	0.897	0.703	0.656	0.986	0.867	0.933
	DSMILES_[R15]	0.906	0.710	0.659	0.987	0.877	0.928
	SELFIES_[R10]	1.000	0.786	0.751	0.974	0.838	0.956
	SELFIES_[R15]	1.000	0.785	0.751	0.974	0.844	0.957
	t-SMILES Family	TS_Vanilla_[R10]	1.000	0.786	0.720	0.991	0.887
TS_Vanilla_[R15]		1.000	0.785	0.713	0.991	0.889	0.909
TSSA_J_[R10]		1.000	0.780	0.762	0.964	0.695	0.977
TSSA_B_[R20]		1.000	0.782	0.751	0.965	0.691	0.960
TSSA_M_[R50]		1.000	0.784	0.764	0.978	0.800	0.975
TSSA_S_[R50]		1.000	0.785	0.768	0.961	0.782	0.978
TSSA_HJBMSV_[R20]		1.000	0.785	0.763	0.958	0.811	0.971
TSDY_B_[R15]		1.000	0.785	0.741	0.983	0.862	0.943
TSDY_M_[R15]		1.000	0.785	0.763	0.950	0.841	0.973
TSDY_S_[R15]		1.000	0.785	0.753	0.979	0.864	0.959
TSDY_HBV_[R15]		1.000	0.786	0.742	0.981	0.881	0.944
TSDY_HMV_[R10]		1.000	0.785	0.759	0.971	0.859	0.966
TSDY_HSV_[R10]		1.000	0.786	0.749	0.979	0.868	0.953
TSDY_HBMSV_[R10]		1.000	0.785	0.759	0.966	0.868	0.967
TSID_B_[R10]		1.000	0.785	0.740	0.984	0.875	0.942
TSID_M_[R10]		1.000	0.785	0.741	0.968	0.884	0.944
TSID_S_[R10]		1.000	0.786	0.735	0.985	0.891	0.936
TSID_HBV_[R15]		1.000	0.786	0.739	0.980	0.867	0.941
TSID_HBMSV_[R10]	1.000	0.786	0.749	0.979	0.870	0.954	

* The results of ORGAN^{3,51}, LSTM^{53,51}, CharacterVAE^{2,51}, AAE^{57,51} and Graph MCTS^{10,51} are taken from GuacaMol⁵¹, Transformer Reg^{40,7} and MGM⁷ are taken from O. Mahmood *et al.*⁷, MolGPT⁴ is taken from Bagal *et al.*⁴, the results of hgraph2graph⁹ is calculated by us. CReM³⁹ is not included as a baseline due to its nearly zero FCD score, even though its novelty score is close to 1. All other models are trained by us. t-SMILES based models are trained in different epochs, with 'R' indicating the training rounds.

Compared to hG2G which is an advanced model based on JTVAE⁸ and aims to solve larger molecular problems with motif-based method, t-SMILES based models have higher FCD scores and lower novelty scores. Compared to MGM, TSSA-based models demonstrate higher scores in novelty, but lower scores in FCD. However, both TSDY and TSID models outperform the MGM model in both novelty and FCD scores.

In the realm of sequence-based baseline models, compared with ORGAN, which is comparable to Graph MCTS with an FCD score approaching zero, t-SMILES based models have markedly higher scores in validity, KLD, FCD and novelty scores, while having a slightly lower score in uniqueness. Compared with AAE, t-SMILES models get higher FCD scores and

lower novelty score. Compared to CharacterVAE, t-SMILES models achieve a lower novelty score, but TSDY and TSID models achieve similar or higher FCD scores.

When evaluating three baseline string representations (SMILES, DSMILES, and SELFIES), SMILES model obtains the highest FCD score of 0.890, SELFIES model attains the lowest FCD score of 0.838, but a higher novelty score of 0.751. DSMILES model achieves lower scores for all five metrics when compared to SMILES.

Comparing three t-SMILES codes, TSSA, TSDY, and TSID, it is clear that TSDY and TSID have higher FCD scores and similar novelty scores compared to TSSA on ChEMBL.

If evaluating t-SMILES and its alternatives, taking the SMILES FCD score of 0.890 as a standard and comparing the novelty score, the TSID_S model achieves an FCD score of 0.891 and a novelty score of 0.735, surpassing SMILES in both dimensions. When the TS_Vanilla model is trained for an additional 5 epochs, it achieves almost the same FCD score as classical SMILES, but it achieves a higher novelty score. Considering the second high FCD score 0.867, which comes from DSMILES, and comparing novelty score, the TSDY_HBV, TSDY_HSV, TSDY_HBSMV, TSID_B, TSID_M, TSID_S, TSID_HBV and TSID_HBSMV 8 t-SMILES models achieve both higher novelty and FCD scores. When the novelty score is set to 0.751, which is the highest in SEMILES, DSMILES and SELFIES, and the FCD score is compared, TSDY_M, TSDY_S, TSDY_HSV, and TSDY_HBMSV achieve both higher novelty and FCD scores. Therefore, it is possible to select and optimize the t-SMILES based models to outperform SMILES, DSMILES, and SELFIES on ChEMBL.

Physicochemical Properties on ChEMBL The detailed results of physicochemical properties are summarized in S1.E.4 and Fig.4.C1-3.

Tables and figures demonstrate that the baseline model hG2G obtains the worst score in six out of nine categories, and the second highest score in another category. Further investigation reveals model hG2G produces more molecules with fewer atoms and rings than the training data, resulting in smaller values for MolWt. However, TSSA_J could almost perfectly match the training data, please refer figures in S1.E.4.1 and S1.E.4.2.

Compared to SMILES, both SELFIES and DSMILES are two points better, but TSID_S outperforms SMILES by 8 out of 9 metrics. With the exception of TSSA_J and TSSA_S, all other t-SMILES models perform a few points better than SMILES. This suggests that many models in the t-SMILES family appear to capture these physicochemical properties better than SMILES, DSMILES, and SELFIES in a similar experiment. Furthermore, the figures and tables indicate that TSDY and TSID models may provide a better fit to the training data compared to TSSA models on ChEMBL.

Goal-Directed Learning We first evaluate t-SMILES codes with a random reconstruction algorithm, using the same default settings as GuacaMol, on twenty sub-tasks. Please refer to SI.B.3.3.3 for comprehensive results. Further in-deep investigation indicates that models based on t-SMILES, as well as its substitutes, are not adequately trained for optimal performance when using the default settings for some sub-tasks. Consequently, this result serves as a point of reference for further research utilizing more training epochs and the goal-directed reconstruction algorithm.

Table SI.B.3.3.3 and figures show that all models could get almost 1.0 scores on the first six subtasks. CReM uses a fragment-based framework that differs from a deep neural network model. It achieves the highest top-two score, with 14 out of 20 tasks. However, it performs poorly in sub-tasks 9, 19, and 20. SELFIES fails to reach any of the top-two highest ratings, while neither SMILES nor TSDY-Scaffold obtain the top-two lowest scores. DSMILES earns only one top-two highest ranking with six top-two lowest rankings.

A comparison of string-based representations shows that DSMILES and SELFIES requires extra optimization to achieve performance comparable to SMILES. In contrast, the t-SMILES family yields diverse higher scores across different sub-tasks.

Goal-directed Reconstruction As a crucial component of t-SMILES framework, besides the random assembly algorithm, we will evaluate three typical subtasks using goal-directed reconstruction algorithm to explore the boundaries of different codes, including 'Median molecules 1' (T9.MM1), 'Sitagliptin MPO' (T16.SMPO), and 'Valsartan SMARTS' (T18.VS). For comparison, we increase the number of training epochs from 20 to 50 for T9.MM1 and T18.VS, and to 100 for T16.SMPO, for better scores. Detailed experiments are presented in Table 4, Fig.5, and SI.B.3.3. CReM achieves the highest scores in SI.B.3.3.3 and serves as the standard in this in-depth evaluation.

The tables and figures show that all models achieve lower scores on T9.MM1 and higher scores on T18.VS. It seems that the target problems are one of the significant factors influencing the results. For molecules with high scores, please refer to SI.B.3.6 and SI.B.3.7. Despite this, the t-SMILES models with goal-directed reconstruction consistently achieve the best performers for both two tasks.

Table 4. Results of Goal-Directed Benchmarks on ChEMBL.

ID	BN	DSs	CReM	SMG	DSG	SFG	TSBR	TSBG	TSSR	TSSG	TSMR	TSMG
9	MM1	0.297	0.360	0.453	0.383	0.410	0.446	0.421	0.443	0.452	0.438	0.467
16	SMPO	0.496	0.708	0.598	0.625	0.725	0.692	0.755	0.693	0.788	0.866	0.930
18	VS	0.258	0.987	0.985	0.988	0.986	0.991	0.987	0.994	0.997	0.985	0.996

*For t-SMILES family, random(R) and goal-directed(G) reconstruction are evaluated. DSs means the scores of training data. 'G' in SMG, DSG and SFG means more training rounds, TS means TSDY. 'R50' means 50 training rounds. 10 or 15 random candidates are selected to calculate scores and the top-scoring one is chosen for output.

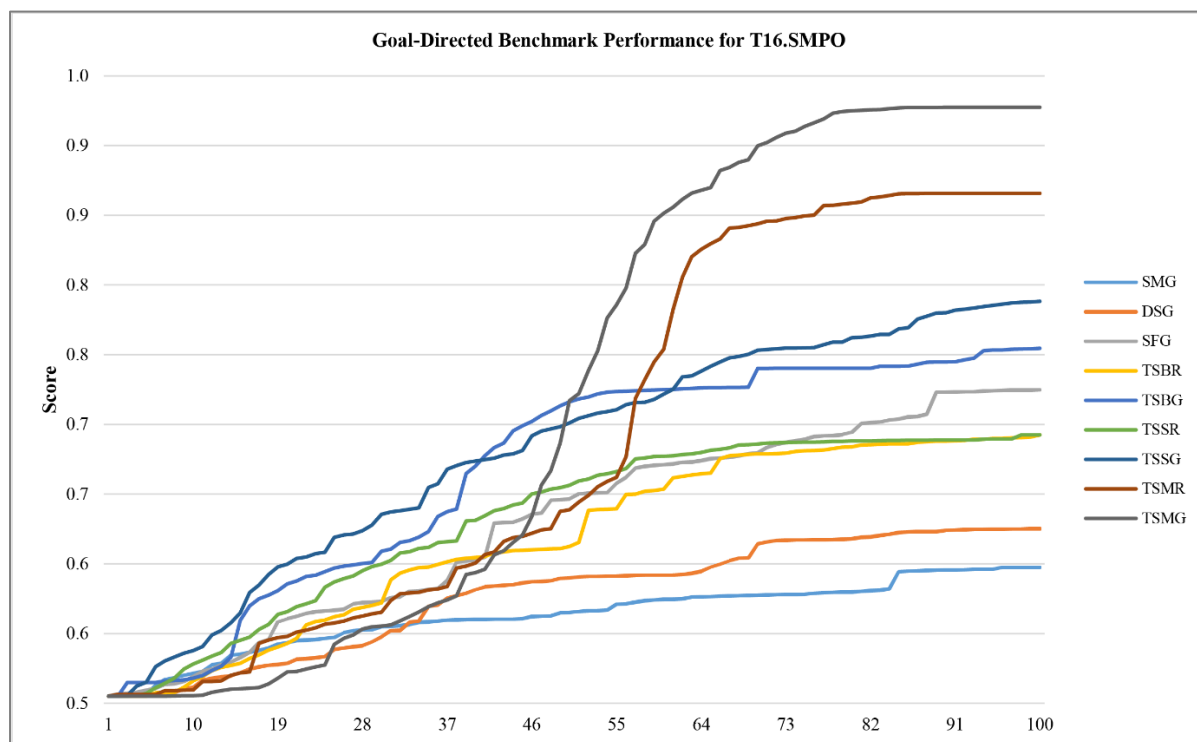


Fig.5 Performance of the Goal-Directed Benchmarks for T16.SMPO with different training epochs. The TSMG model yields significantly high results. For further comprehensive experiments and nuanced discussions, please refer to section SI.B.3.4.

Regarding T16.SMPO, additional experiments and analysis are conducted as presented in Fig.5, SI.Fig.B.3.3.4.1 and SI.Fig.B.3.3.4.2. All six t-SMILES-based models significantly outperform SMILES-based models. In particular, among the models tested, TSDY_M models achieve significantly higher scores on this specific task. These findings suggest that t-SMILES could have further applicability in reaching the target function's limit, and ultimately help chemists create more rational target functions. Please refer to SI.B.3.4 for further experiments and analyses.

Furthermore, from figures in SI.B.3.3.5 and SI.B.3.3.6 one can see that there is significant variation in physicochemical properties beyond the target properties across models for T18.VS. Meanwhile, SI.B.3.3.8 shows also a noteworthy difference among molecules with different scores in different codes regarding T16.SMPO. Therefore, in practical experiments to ensure

more favorable results in goal-directed tasks, it is advised to use singleton or hybrid t-SMILES model, which best suits the given task and is well optimized.

Experiments on Zinc

Distribution Learning As shown in Table 5, from the comparative analysis of baseline models, the t-SMILES based models in this study significantly outperform the fragment-based baseline models. JTVAE⁸ is one key baseline model for this study. So far as the validity is concerned, both t-SMILES and JTVAE⁸ models could generate almost 100% valid molecules. However, t-SMILES exhibits significantly higher KLD and FCD scores with reasonably slightly lower novelty and uniqueness scores.

t-SMILES based models significantly outperforms another fragment dictionary-based model, FragDgm²⁶, which splits molecule in a linear mode as a sequence of fragment IDs, on all five distribution parameters. Although FragDgm uses a segmented mode and being based on distributional learning, its FCD value is the lowest of all listed models.

As to Group-VAE²⁸, which uses fragments and SELFIES, it achieves a lower score in novelty compared to SELFIES-VAE in published experiments. And, SELFIES based GPT model obtained lower scores for both novelty and FCD compared to the five t-SMILES based models in this experiment. Group-VAE use a different way to calculate FCD making it impossible to make a direct comparison.

In terms of string descriptions, the DSMILES model achieves the highest FCD score of 0.930 and the lowest validity and novelty scores. The SELFIES model is able to generate 100% valid molecules and has almost the same novelty score as SMILES; however, it achieves the lowest FCD score of 0.915 among the three models.

To evaluate the t-SMILES family with its alternatives, we fix the FCD score 0.923 of SMILES and compare the novelty, TSDY_S and TSDY_HBMSV get similar FCD score and higher novelty score. Considering the highest novelty score 0.767, six models TSDY_S, TSDY_HBV, TSDY_HSV, TSDY_HBMSV, TSID_B and TSID_HBV could get higher FCD scores. When comparing the novelty score, only TS_Vanilla and TSDY_B get lower scores, other 13 models get higher novelty scores than SMILES. It means that t-SMILES models, with almost 100% validity and relatively high FCD scores, could improve novelty to explore a wider molecular space. That is to say, t-SMILES is an effective molecular representation for fragment based molecular tasks on Zinc.

Table 5. Results for the Distribution-Learning Benchmarks on Zinc using GPT.

	Model	Valid	Unique	Novelty	KLD	FCD	Nov./Uni.
Baseline Models	JTVAE ⁸	0.997	0.989	0.989	0.870	0.439	1.000
	FragDgm ²⁶	1.000	0.423	0.422	0.835	0.303	0.998
	BRICS_Random	1.000	0.796	0.796	0.953	0.641	1.000
	MolGPT ⁴	0.994	1.000	0.797	N/A	N/A	N/A
	SELFIES-VAE ²⁸	1.000	0.999	0.735	N/A	N/A	N/A
	Group-VAE ²⁸	1.000	0.999	0.719	N/A	N/A	N/A
String Rep	SMILES	0.980	0.770	0.766	0.989	0.923	0.995
	DSMILES	0.962	0.756	0.736	0.992	0.930	0.974
GPT	SELFIES	1.000	0.786	0.767	0.988	0.915	0.976
t-SMILES Family GPT	TS_Vanilla	1.000	0.786	0.760	0.993	0.902	0.967
	TSSA_J	1.000	0.783	0.780	0.984	0.823	0.996
	TSSA_B	1.000	0.782	0.776	0.965	0.716	0.992
	TSSA_M	1.000	0.783	0.778	0.984	0.842	0.993
	TSSA_S	1.000	0.786	0.783	0.951	0.829	0.997
	TSSA_HJBMSV	1.000	0.785	0.783	0.965	0.874	0.997
	TSDY_B	1.000	0.786	0.762	0.990	0.917	0.970
	TSDY_M	1.000	0.786	0.778	0.982	0.903	0.990
	TSDY_S	1.000	0.786	0.774	0.989	0.921	0.985
	TSDY_HBV	1.000	0.786	0.770	0.991	0.914	0.980
	TSDY_HMV	1.000	0.786	0.779	0.986	0.911	0.991
	TSDY_HSV	1.000	0.786	0.775	0.992	0.919	0.987
	TSDY_HBMSV	1.000	0.786	0.779	0.983	0.922	0.992
	TSID_B	1.000	0.786	0.767	0.988	0.917	0.976
	TSID_HBV	1.000	0.786	0.773	0.991	0.917	0.983

*MolGPT⁴ is taken from Bagal *et al.*⁴, SELFIES-VAE²⁸ and Group-VAE²⁸ are taken from Cheng *et al.*²⁸. All other models are trained by us. ‘MolGPT’ means the same setting of MolGPT⁴ is used. BRICS_Random model assembles BRICS-based fragments randomly. TS based models are trained in 50 epochs.

Physicochemical Properties on Zinc S.I.E.5 and Fig.4.Z1-3 show that none of the three baseline models JTVAE⁸, FragDgm²⁶, and BRICS_Rnd achieve better scores than SMILES. FragDgm achieves the worst scores in six out of nine categories.

JTVAE⁸, gets the worst scores in three out of nine categories. Further investigation shows that the JTVAE⁸ model produces more molecules with fewer atoms and rings than the training data, resulting in smaller values for MolWt. However, TSSA_J was able to match the training data almost perfectly as shown in S.I.E.5.1 and S.I.E.5.2. Another baseline model, FragDgm, has more average values for the number of atoms and rings that are far from the training data. As a result, JTVAE⁸ and FragDgm are the worst at learning patterns from the training data.

On the contrary, DSMILES, SELFIES, TS_Vanilla, TSDY_S, TSDY_HBV, TSDY_HSV, and TSID_HBV get five to seven points better scores than SMILES. Based on these results, some t-SMILES models, DSMILES, and SELFIES are able to capture these physiochemical properties as effectively as SMILES in these experiments. Conversely, FragDgm and JTVAE⁸ show limited capabilities.

Experiments on QM9

As illustrated in SI.Table.E.6 and SI.Fig.E.6.2, all of the string-based QM9 models including t-SMILES, SMILES, DSMILES and SEFLIES except for CharacterVAE, achieve FCD scores close to or greater than 0.96, while having reasonably lower novelty scores. Our approach performs better than existing string-based approaches. Compared to graph-based baseline models, our approach demonstrates superior performance. TSSA_J generates more molecules with greater molecular weights, likely because these molecules contain more atoms. Therefore, TSSA_J yields higher novelty scores in all t-SMILES models. For a comprehensive analysis of distribution learning and physicochemical properties metrics, please refer to SI.E.6.

Discussion

When using advanced NLP methodologies to solve chemical problems, two fundamental questions arise: 1) What are 'chemical words'? and 2) How can they be encoded as 'chemical sentences'? This study introduces a framework called t-SMILES to address the second question. t-SMILES utilizes BFS to encode fragmented molecules as a string. Instead of using dictionary ID, classical SMILES is used to describe the fragment. This means that, t-SMILES can build a multiscale string-based molecular representation, simplifying the computational complexity and enhancing the background knowledge, since the molecular structure is locally correlated in nature. This significantly reduces the nesting depth and the difficulty of AI models to capture long-range dependencies in the grammar.

Systematic comparison experiments indicate that DSMILES and SELFIES require further optimization to match the performance of SMILES on some tasks due to their advanced grammar, as summarized by M. Krenn et al. In contrast, compared to classical SMILES, t-SMILES introduces only two additional symbols, '&' and '^', to encode multi-scale and hierarchical molecular topology. Due to their resemblances, it is relatively straightforward to optimize t-SMILES based models to surpass classical SMILES, especially TSDY and TSID.

Three code algorithms are presented in this work: TSSA, TSDY, and TSID. TSSA has the highest reconstruction novelty score, while TSDY and TSID provide a more accurate fit of the physicochemical properties of training data with higher generative novelty scores. Furthermore, both random and goal-oriented reconstruction algorithms are evaluated. The latter significantly outperforms SOTA baseline models in goal-directed learning tasks. In addition, t-SMILES offer a wider range of advantages, especially for data sets with limited resources, achieving higher scores to balance novelty and FCD.

Furthermore, the t-SMILES framework has the ability to unify classical SMILES as TS-Vanilla, making t-SMILES a superset of SMILES to build a multi-code molecular description system. When inspecting organic molecules, complex patterns are often recognized, which are more intricate than individual groups. Therefore, in real-world molecule modeling tasks, it is recommended to use hybrid t-SMILES approaches to explore as much of the chemical space as possible or a singleton t-SMILES model for a specific task. Moreover, t-SMILES make it possible to generate valid and chemically diverse fragments which can be served as foundation for other fragment-based researches.

Scalability Theoretically, t-SMILES algorithm is capable of supporting any effective substructure types and patterns as long as they can be used to obtain chemically valid molecular fragments. With the invaluable accumulation of drug fragments by experienced chemists, t-SMILES algorithm can combine this experience with a powerful sequence-based deep neural network model to help chemists better exploring their experimental space.

In addition, t-SMILES is an open and flexible framework for encoding fragmented molecules using tree-based algorithms. If we use SMILES to encode the fragments, we get the t-SMILES string. If we use DSMILES or SELFIES to encode the fragments, we will get the t-DSMILES or t-SELFIES strings.

In some special cases, the t-SMILES algorithm could encode tree nodes by dictionary id instead of SMILES if only a specific fragment space needs to be explored and no expansion is required. Alternatively, we could replace the newly generated fragments with the fragments from the training data according to a given set of rules. In these cases, the coding logic and the flow of the algorithm of t-SMILES will remain unchanged.

Limitation and to be improved Large Language Models (LLMs) have recently demonstrated impressive reasoning abilities in various tasks. And some research has shown that LLMs can understand well-formed English syntax. So, whether the tree structure of t-SMILES could be learned and how LMs go beyond superficial statistical correlations to learn the chemical knowledge of molecules remains to be explored in depth.

This work focused on encoding fragmented molecules as sequence, so only published fragmentation algorithms are used as examples to create ‘chemical words’. Future research could utilize t-SMILES to explore additional fragmentation algorithms and decipher chemical sentences and meanings more deeply.

The results of our experiments show that both the assembly and optimization algorithms have an impact on the quality of the assembled molecules. This could be a starting point for further research in this challenging area.

Although t-SMILES aims to improve the performance of molecule description with some modifications to the original SMILES model to circumvent its limitations, experiments on more complex molecules were not performed in this study. This will be a topic for future research.

Finally, in addition to the GPT and LSTM, further research could explore enhanced generative models, evolutionary techniques, as well as property, retrosynthesis, and reaction prediction tasks.

Reference

1. Jiménez-Luna, J., Grisoni, F. & Schneider, G. Drug discovery with explainable artificial intelligence. *Nature Machine Intelligence* vol. 2 573–584 (2020).
2. Gómez-Bombarelli, R. *et al.* Automatic Chemical Design Using a Data-Driven Continuous Representation of Molecules. *ACS Cent. Sci.* **4**, 268–276 (2018).
3. Guimaraes, G. L., Sánchez-Lengeling, B., Farias, P. L. C. & Aspuru-Guzik, A. Objective-Reinforced Generative Adversarial Networks (ORGAN) for Sequence Generation Models. *ArXiv* **abs/1705.1**, (2017).
4. Bagal, V., Aggarwal, R., Vinod, P. K. & Priyakumar, U. D. MolGPT: Molecular Generation Using a Transformer-Decoder Model. *J. Chem. Inf. Model.* **acs.jcim.1c00600** (2021) doi:10.1021/acs.jcim.1c00600.
5. Weininger, D. SMILES, a Chemical Language and Information System: 1: Introduction to Methodology and Encoding Rules. *J. Chem. Inf. Comput. Sci.* **28**, 31–36 (1988).
6. Xia, X., Hu, J., Wang, Y., Zhang, L. & Liu, Z. Graph-based generative models for de Novo drug design. *Drug Discov. Today Technol.* **32–33**, 45–53 (2019).
7. Mahmood, O., Mansimov, E., Bonneau, R. & Cho, K. Masked graph modeling for molecule generation. *Nat. Commun.* **12**, 1–36 (2021).
8. Jin, W., Barzilay, R. & Jaakkola, T. Junction Tree Variational Autoencoder for Molecular Graph Generation. in *International conference on machine learning* vols. 2021-Janua 2323–2332 (PMLR, 2018).
9. Hu, Y., Hu, Y. & Cen, E. Hierarchical Generation of Molecular Graphs using Structural Motifs. *Proc. - 2021 2nd Int. Conf. Big Data Artif. Intell. Softw. Eng. ICBASE 2021* 543–546 (2021) doi:10.1109/ICBASE53849.2021.00106.
10. Jensen, J. H. A graph-based genetic algorithm and generative model/Monte Carlo tree search for the exploration of chemical space. *Chem. Sci.* **10**, 3567–3572 (2019).
11. Hoogeboom, E., Satorras, V. G., Vignac, C. & Welling, M. Equivariant Diffusion for

- Molecule Generation in 3D. *ArXiv* (2022).
12. Bodnar, C. *et al.* Weisfeiler and Lehman go cellular: CW networks. *Adv. Neural Inf. Process. Syst.* **34**, 2625–2640 (2021).
 13. Bouritsas, G., Frasca, F., Zafeiriou, S. & Bronstein, M. Improving Graph Neural Network Expressivity via Subgraph Isomorphism Counting. *ArXiv* **abs/2006.0**, (2020).
 14. Bodnar, C. *et al.* Weisfeiler and lehman go topological: Message passing simplicial networks. in *International Conference on Machine Learning* 1026–1037 (PMLR, 2021).
 15. Wu, Z. *et al.* A Comprehensive Survey on Graph Neural Networks. *IEEE Trans. Neural Networks Learn. Syst.* **32**, 4–24 (2021).
 16. Skinnider, M., Stacey, R. G., Wishart, D. & Foster, L. Chemical language models enable navigation in sparsely populated chemical space. *Nat. Mach. Intell.* **3**, 759–770 (2021).
 17. O’Boyle, N. M. & Dalke, A. DeepSMILES: An adaptation of SMILES for use in machine-learning of chemical structures. *ChemRxiv* 1–9 (2018) doi:10.26434/CHEMRXIV.7097960.V1.
 18. Arús-Pous, J. *et al.* Randomized SMILES strings improve the quality of molecular generative models. *J. Cheminform.* **11**, 1–13 (2019).
 19. Krenn, M. *et al.* SELFIES and the future of molecular string representations. *Patterns* **3**, (2022).
 20. Krenn, M., Häse, F., Nigam, A., Friederich, P. & Aspuru-Guzik, A. Self-Referencing Embedded Strings (SELFIES): A 100% robust molecular string representation. *Mach. Learn. Sci. Technol.* **1**, 045024 (2019).
 21. Lecun, Y., Bengio, Y. & Hinton, G. Deep learning. *Nature* vol. 521 436–444 (2015).
 22. Mitrovic, J., McWilliams, B., Walker, J., Buesing, L. & Blundell, C. Representation Learning via Invariant Causal Mechanisms. *ICML* 1–21 (2020).
 23. Maziarz, K. *et al.* Learning to Extend Molecular Scaffolds with Structural Motifs. 1–22 (2021).
 24. Zhang, Z., Liu, Q., Wang, H., Lu, C. & Lee, C.-K. Motif-based Graph Self-Supervised Learning for Molecular Property Prediction. *ArXiv* **abs/2110.0**, (2021).
 25. Yu, Z. & Gao, H. Molecular Representation Learning via Heterogeneous Motif Graph Neural Networks. (2022).
 26. Podda, M., Bacciu, D. & Micheli, A. A deep generative model for fragment-based molecule generation. in *International Conference on Artificial Intelligence and*

- Statistics* 2240–2250 (PMLR, 2020).
27. Jin, W., Barzilay, R. & Jaakkola, T. Multi-Objective Molecule Generation using Interpretable Substructures. *37th Int. Conf. Mach. Learn. ICML 2020 Part F16814*, 4799–4809 (2020).
 28. Cheng, A. H. *et al.* Group SELFIES: a robust fragment-based molecular string representation. *Digit. Discov.* **2**, 748–758 (2023).
 29. Butler, K., Davies, D. W., Cartwright, H., Isayev, O. & Walsh, A. Machine learning for molecular and materials science. *Nature* (2018) doi:10.1038/s41586-018-0337-2.
 30. Schneider, P. *et al.* Rethinking drug design in the artificial intelligence era. *Nat. Rev. Drug Discov.* **19**, 353–364 (2019).
 31. Lehn, J.-M. Supramolecular chemistry — Scope and perspectives: Molecules — Supermolecules — Molecular devices. *J. Incl. Phenom.* **6**, 351–396 (1988).
 32. Jean-Marie Lehn - Interview.
<https://www.nobelprize.org/prizes/chemistry/1987/lehn/interview/>.
 33. Cadeddu, A., Wylie, E. K., Jurczak, J., Wampler-Doty, M. & Grzybowski, B. A. Organic chemistry as a language and the implications of chemical linguistics for structural and retrosynthetic analyses. *Angew. Chemie Int. Ed.* **53**, 8108–8112 (2014).
 34. Ip, Y. T. & Davis, R. J. Signal transduction by the c-Jun N-terminal kinase (JNK) - From inflammation to development. *Curr. Opin. Cell Biol.* **10**, 205–219 (1998).
 35. AID 1706 - QFRET-based primary biochemical high throughput screening assay to identify inhibitors of the SARS coronavirus 3C-like Protease (3CLPro) - PubChem.
<https://pubchem.ncbi.nlm.nih.gov/bioassay/1706>.
 36. Degen, J., Wegscheid-Gerlach, C., Zaliani, A. & Rarey, M. On the art of compiling and using “drug-like” chemical fragment spaces. *ChemMedChem* **3**, 1503–1507 (2008).
 37. Hussain, J. & Rea, C. Computationally efficient algorithm to identify matched molecular pairs (MMPs) in large data sets. *J. Chem. Inf. Model.* **50**, 339–348 (2010).
 38. Bemis, G. W. & Murcko, M. A. The properties of known drugs. 1. Molecular frameworks. *J. Med. Chem.* **39**, 2887–2893 (1996).
 39. Polishchuk, P. CReM: chemically reasonable mutations framework for structure generation. *J. Cheminform.* **12**, (2020).
 40. Vaswani, A. *et al.* Attention is all you need. *Adv. Neural Inf. Process. Syst.* **2017-Decem**, 5999–6009 (2017).
 41. Flam-Shepherd, D., Zhu, K. & Aspuru-Guzik, A. Language models can learn complex

- molecular distributions. *Nat. Commun.* **13**, 1–10 (2022).
42. Lounkine, E., Batista, J. & Bajorath, J. Random Molecular Fragment Methods in Computational Medicinal Chemistry. *Curr. Med. Chem.* **15**, 2108–2121 (2008).
 43. Landrum, G. RDKit: A software suite for cheminformatics, computational chemistry, and predictive modeling. *Greg Landrum* (2013).
 44. Rarey, M. & Dixon, J. S. Feature trees: A new molecular similarity measure based on tree matching. *J. Comput. Aided. Mol. Des.* **12**, 471–490 (1998).
 45. Ertl, P., Schuffenhauer, A. & Renner, S. Reduced Graphs and Their Applications in Chemoinformatics. *Life Sci.* **672**, 588 (2011).
 46. Takahashi, Y., Sukekawa, M. & Sasaki, S. ichi. Automatic Identification of Molecular Similarity Using Reduced-Graph Representation of Chemical Structure. *J. Chem. Inf. Comput. Sci.* **32**, 639–643 (1992).
 47. Rarey, M. & Stahl, M. Similarity searching in large combinatorial chemistry spaces. *J. Comput. Aided. Mol. Des.* **15**, 497–520 (2001).
 48. Leach, A. R. & Gillet, V. J. *An introduction to cheminformatics. An Introduction To Cheminformatics* (Springer, 2007). doi:10.1007/978-1-4020-6291-9.
 49. Gao, W., Mercado, R. & Coley, C. W. Amortized Tree Generation for Bottom-up Synthesis Planning and Synthesizable Molecular Design. *arXiv Prepr. arXiv2110.06389* (2021).
 50. Nguyen, D. H. & Tsuda, K. A generative model for molecule generation based on chemical reaction trees. 1–12 (2021).
 51. Brown, N., Fiscato, M., Segler, M. H. S. & Vaucher, A. GuacaMol: Benchmarking Models for De Novo Molecular Design. *J. Chem. Inf. Model.* **59** **3**, 1096–1108 (2019).
 52. Singh, S. & Mahmood, A. The NLP Cookbook: Modern Recipes for Transformer Based Deep Learning Architectures. *IEEE Access* **9**, 68675–68702 (2021).
 53. Hochreiter, S. & Schmidhuber, J. Long Short-Term Memory. *Neural Comput.* **9**, 1735–1780 (1997).
 54. Mordatch, I. MOG: MOLECULAR OUT-OF-DISTRIBUTION GENERATION WITH ENERGY-BASED MODELS. 1–6 (2018).
 55. Erlanson, D. A., Fesik, S. W., Hubbard, R. E., Jahnke, W. & Jhoti, H. Twenty years on: The impact of fragments on drug discovery. *Nat. Rev. Drug Discov.* **15**, 605–619 (2016).
 56. Xiong, Z. *et al.* Pushing the boundaries of molecular representation for drug discovery with the graph attention mechanism. *J. Med. Chem.* **63**, 8749–8760 (2020).

57. Makhzani, A., Shlens, J., Jaitly, N., Goodfellow, I. & Frey, B. Adversarial Autoencoders. (2015).